NUMERICAL SIMULATION OF THE FLOW-INDUCED VIBRATION IN THE FLOW AROUND TWO CIRCULAR CYLINDERS IN TANDEM ARRANGEMENTS

Bruno Carmo, Spencer Sherwin, Peter Bearman
Department of Aeronautics, Imperial College London, UK
Richard Willden
Department of Engineering Science, University of Oxford, UK

ABSTRACT

In this paper, the effect of wake interference on the flow-induced vibrations of circular cylinders is investigated. Two- and three-dimensional computational simulations of the fluid-structure interaction in the flow around two cylinders in tandem arrangements are performed. The Reynolds numbers are 150 for the two-dimensional simulations and 300 for the three-dimensional simulations. The upstream cylinder is fixed and the downstream cylinder is mounted on a elastic base of small mass and damping. The results show that the structural response in the tandem arrangements is remarkably different from that of the single cylinder; higher amplitudes and broader lock-in regions are observed in the flow around the pairs of cylinders.

1. INTRODUCTION

The flow-induced vibration of cylindrical structures is a key engineering issue. In many situations it is common to find multiple cylinders placed in close proximity to one another, such that the flow field, fluid forces and, consequently, structural response of each cylinder can be quite different from those observed for an isolated cylinder. The influence of the presence of one cylinder on the flow field about the other is known as flow interference.

When two fixed identical circular cylinders are placed in a tandem arrangement, it is found that the downstream cylinder experiences cross-stream lift forces dramatically higher than those experienced by an isolated cylinder (Mahbub Alam et al., 2003; Carmo, 2005). To understand how the approaching wake interacts with a compliant body, we investigated the flow around a circular cylinder mounted on an elastic basis, allowed to move only in the transverse direction, immersed in the wake of an upstream fixed circular cylinder of the same diameter, as sketched in figure 1.

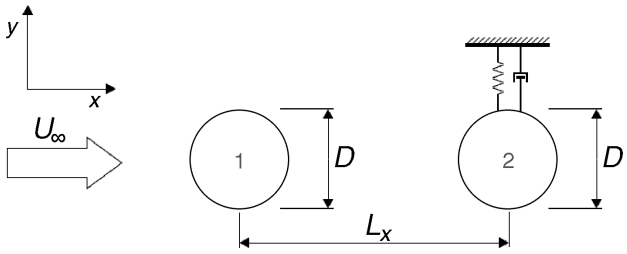

Figure 1: *Schematic drawing of investigated arrangement.*

To our knowledge, no previous work on this configuration using computational simulation has been published. In the present study, two- and three-dimensional numerical simulations were carried out to investigate this particular case of fluid-structure interaction.

2. METHODOLOGY

The incompressible fluid flow was simulated by solving the incompressible Navier-Stokes equations, which were discretized using the high accuracy Spectral/hp element method (Karniadakis and Sherwin, 2005). Specifically for the three-dimensional simulations, a Fourier expansion discretisation was used in the spanwise direction (Karniadakis, 1990). A stiffly stable time splitting scheme (Karniadakis et al., 1991) was employed to advance the solution in time. Because the two cylinders have non-zero relative displacement in time, the method had to allow for domain deformation. Therefore, an Arbitrary Lagrangean-Eulerean (ALE) scheme was incorporated into the code. Following Batina (1990), the mesh was adapted to the boundary displacement in every time step by modelling each mesh element edge by a spring with stiffness inversely proportional to its length. The mesh movement

was coupled to the time splitting scheme in a similar fashion as detailed in Beskok and Warburton (2001).

The dynamics of the downstream cylinder was modelled as a one-dimensional linear mass-spring-damper system. The cylinder was able to move in the transverse direction only. The structural equation was integrated using Newmark's scheme (Newmark, 1959) and was loosely coupled to the time stepping scheme of the flow solver (Jester and Kallinderis, 2004).

3. NUMERICAL SIMULATIONS

Two- and three-dimensional numerical simulations were performed considering the flow around the geometrical configuration sketched in figure 1. The structural parameters of the elastic base were $m* = 2.0$ and $\zeta = 0.007$. The reduced velocities ($Vr = U/(f_n D)$, where U is the free-stream velocity, f_n the natural frequency of the elastic base in vacuum and D the cylinder diameter) tested ranged from 3.0 to 30.0, and it was varied by changing the spring stiffness and keeping the Reynolds number ($Re = UD/\nu$, where ν is the kinematic viscosity of the fluid) constant. The Reynolds number was 150 for the two-dimensional simulations and 300 for the three-dimensional simulations. The configurations tested were $L_x/D = 1.5$, 3, 5 and 8.

Besides the simulations of the flow around tandem arrangements, simulations of the flow around a single cylinder mounted on an elastic base with the same structural parameters were performed, to serve as a benchmark for comparisons.

4. TWO-DIMENSIONAL RESULTS

4.1. Single cylinder results

The results obtained for the flow around a single cylinder, pictured in figure 2, show the typical response of vortex-induced vibrations at low Reynolds numbers and low mass ratio (for comparison, see, for example, Singh and Mittal, 2005; Willden and Graham, 2006). There is a very well defined lock-in region, where the vortex shedding frequency locks to a value close to the natural frequency of the structure, as can be seen in the frequency plot in figure 2. It is in this region that the amplitudes are highest, reaching a maximum value of $A/D = 0.582$ for the cases investigated, and it is also there that the phase angle ϕ changes from a value close to 0° to a value close to 180°.

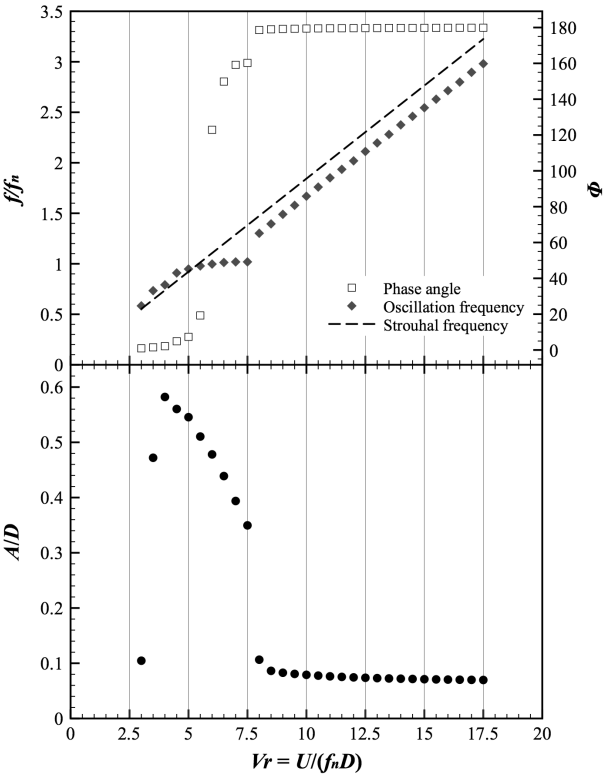

Figure 2: *Non-dimensional amplitude (A/D), phase angle (ϕ) and frequency plots against reduced velocity for the flow around an isolated cylinder, $Re = 150$, two-dimensional simulations. The Strouhal frequency is the vortex shedding frequency in the flow around a fixed cylinder at the same Reynolds number.*

For $V_r \geq 8.0$ the amplitude of vibration always give low values ($A/D < 0.1$), and the phase angle is close to 180°.

4.2. Small separations

The structural responses in the two-dimensional simulations for the configurations $L_x/D = 1.5$ and $L_x/D = 3.0$ were very similar; figure 3 shows the results for $L_x/D = 3.0$. There is not a well defined lock-in region, as in the single cylinder case. The amplitude of vibration reaches a peak for a reduced velocity between 5 and 7.5 and decrease smoothly afterwards, instead of showing the abrupt decrease observed for the single cylinder case. For reduced velocities from 15 up to 30, the amplitude of vibration is surprisingly high (between $0.4D$ and $0.5D$), although the phase angle is close to 180°.

Regarding the frequency of vibration, also shown in figure 3, it can be seen that for the first few points the frequency follows the Strouhal

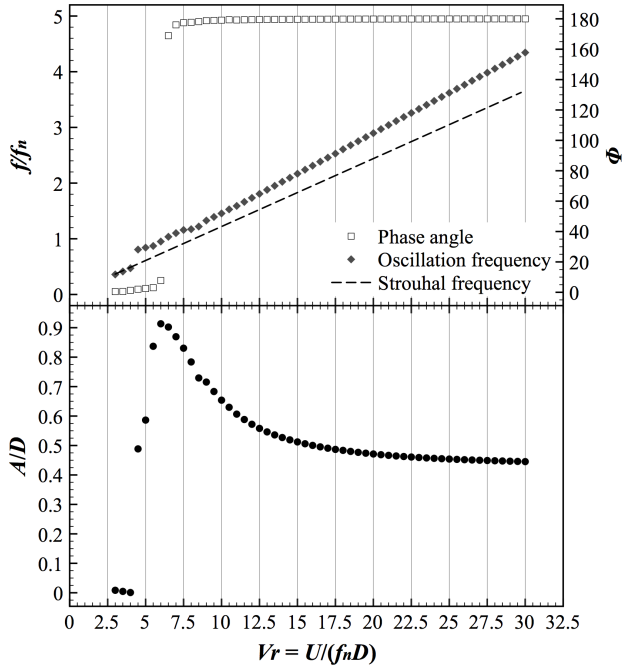

Figure 3: *Amplitude, phase angle and frequency plots against reduced velocity for the flow around two cylinders in tandem,* $L_x/D = 3$*,* $Re = 150$*, two-dimensional simulations.*

line, but they stop coinciding as soon as the amplitude of vibration becomes high and the points end up following a linear trend with positive slope, which is different from that of the Strouhal line for the fixed arrangement. This can be understood by looking at the vorticity contours in figure 4. Once the downstream cylinder started to vibrate with a reasonable amplitude, the shedding regime changed completely from what was observed when the cylinders were fixed, and so did the main frequency of the flow.

With this change of regime the third harmonic of the force signal has strong energy even at high reduced velocities. The third harmonic appeared because the force acting on the downstream cylinder had two different sources, and they acted with the same frequency but different phase and amplitude. The first source was the vortices generated by the upstream cylinder that impinge on the downstream cylinder, and the second was the vortices shed by the downstream cylinder. These sources are tightly linked, which is why they had the same frequency, but they had their maxima at different moments during the oscillation cycle. The graph in figure 5 shows the downstream cylinder lift coefficient and displacement spectra, for $Vr = 15.0$. It can be noticed that even for such a high value of reduced velocity, the odd harmonics of the lift force do have

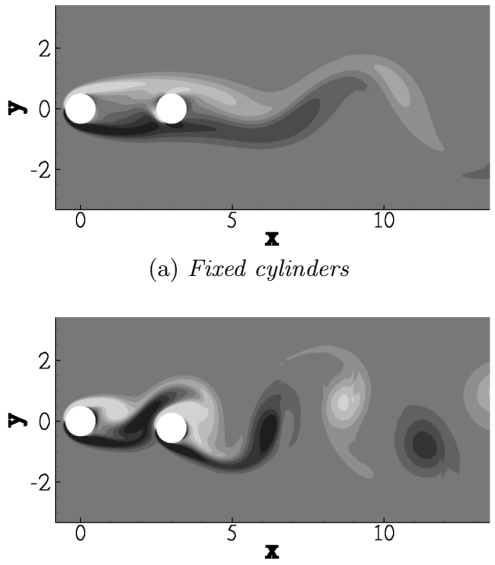

(a) *Fixed cylinders*

(b) $Vr = 10.0$

Figure 4: *Instantaneous vorticity contours illustrating different shedding regimes.* $L_x/D = 3$*,* $Re = 150$*, two-dimensional simulations.*

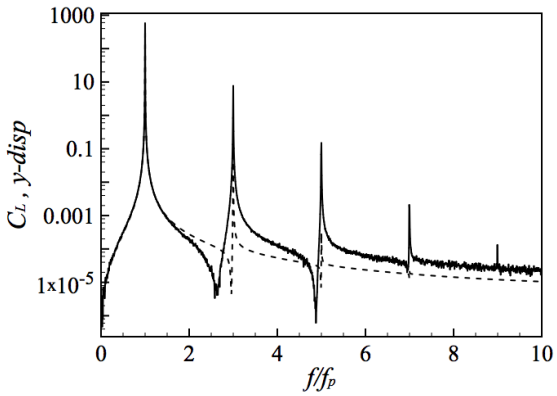

Figure 5: *Downstream cylinder lift coefficient (solid lines) and displacement (dashed lines) spectra.* $L_x/D = 3$*,* $Re = 150$*,* $Vr = 15.0$*, two-dimensional simulations.*

high energy.

4.3. Large separations

For the larger separations investigated, $L_x/D = 5$ and $L_x/D = 8$, the system response differed from what was observed for a single cylinder and for the small separations. The results for $L_x/D = 8$ are shown in figure 6; the results for $L_x/D = 5$ were similar and are not shown here due to space limitation. First of all there is a lock-in region, in the sense that the cylinder vibrates at a frequency close to the structural natural frequency, instead of following the Strouhal

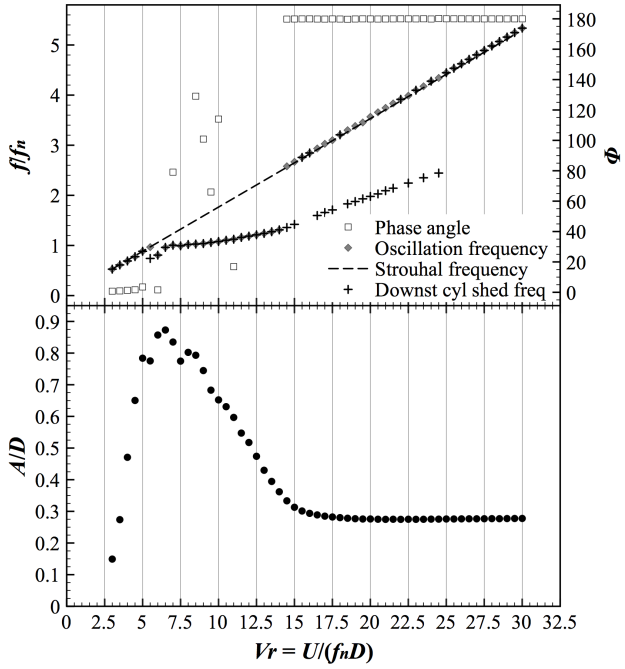

Figure 6: *Amplitude, phase angle and frequency plots against reduced velocity for the flow around two cylinders in tandem,* $L_x/D = 8$*,* $Re = 150$*, two-dimensional simulations.*

frequency, for a certain range. In this region, the shedding from the downstream cylinder has a strong component at the natural frequency of the structure. It can be seen that this region is much larger for $L_x/D = 8$ than for the single cylinder case, reaching reduced velocities as high as 15.0. Another difference is that the transition between the lock-in and the higher Vr regime happens smoothly, and not abruptly as in the single cylinder case. Another evident feature is a secondary peak, appearing where the Strouhal frequency is approximately equal to $1.5f_n$. For higher reduced velocities, the oscillation amplitude tends to a value higher than that observed for the single cylinder case, but lower than those observed for the small separations. Regarding the shedding frequency, it can be seen in figure 6 that, for the larger separations, the shedding from the upstream cylinder follows the Strouhal line.

In figure 6 only the frequency with the highest energy is plotted. However, if we consider the force and displacement spectra of one of the cases as for example in figure 7, we can see that these spectra have many other important frequencies, as opposed to the rather clean spectra plotted in figure 5. Also the time histories of the lift coefficient and displacement are not regular, as can be seen in figure 8. It seems that the wake coming from the upstream cylinder makes the flow-structure interaction much more complex, even for this low Reynolds number. Since the force acting on the downstream cylinder has a broad range of frequencies with high energy, the cylinder will respond to the frequency closest to its natural frequency, and that is why a much larger lock-in region is observed. For all reduced velocities, at least two dominant peaks in the displacement spectrum were observed: one being at the natural frequency and the other being at the Strouhal frequency.

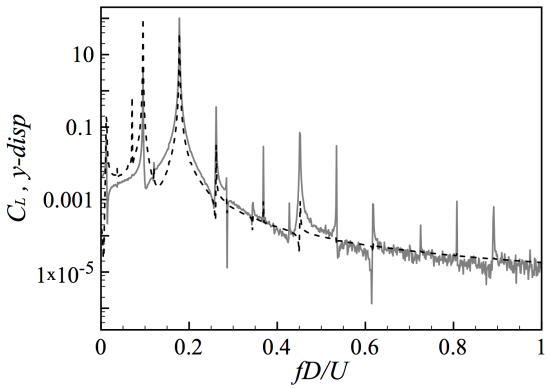

Figure 7: *Downstream cylinder lift coefficient (solid lines) and displacement (dashed lines) spectra.* $L_x/D = 8.0$*,* $Vr = 13.0$*,* $Re = 150$*, two-dimensional simulations.*

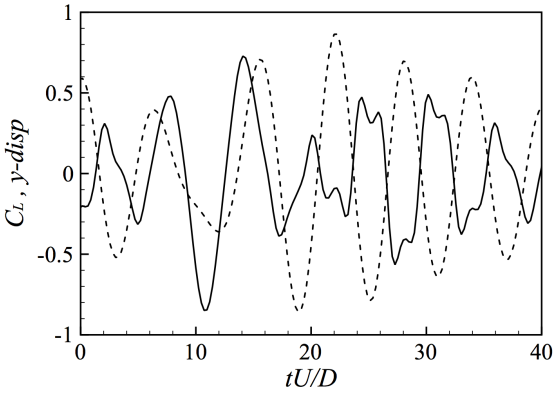

Figure 8: *Downstream cylinder lift coefficient (solid lines) and displacement (dashed lines) time series.* $L_x/D = 8.0$*,* $Re = 150$*,* $Vr = 6.5$ *two-dimensional simulations.*

When the reduced velocity is close to the first peak, what was observed is that the phase angle jumped intermittently from a value close to 0° to a value close to 180°, as can be seen in the time histories plotted in figure 8. This suggests that the inherent non-linearity of the system prevents it getting to a stable equilibrium point, and the system keeps alternating between two transient

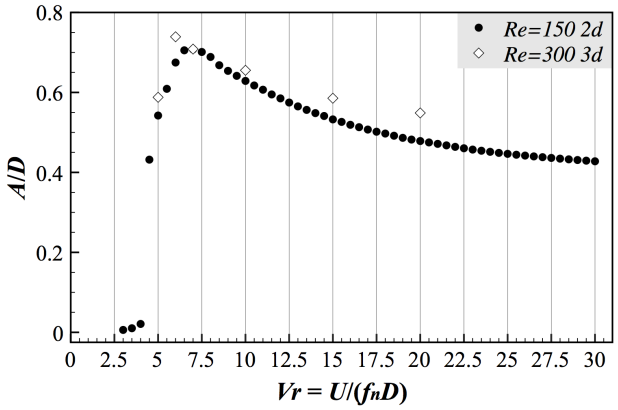

(a) $L_x/D = 1.5$

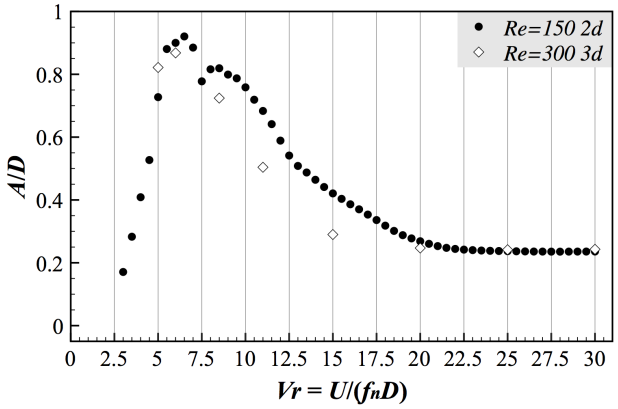

(b) $L_x/D = 5$

Figure 9: *Comparison between the amplitude of vibration obtained from two- (closed symbols) and three-dimensional (open symbols) simulations.*

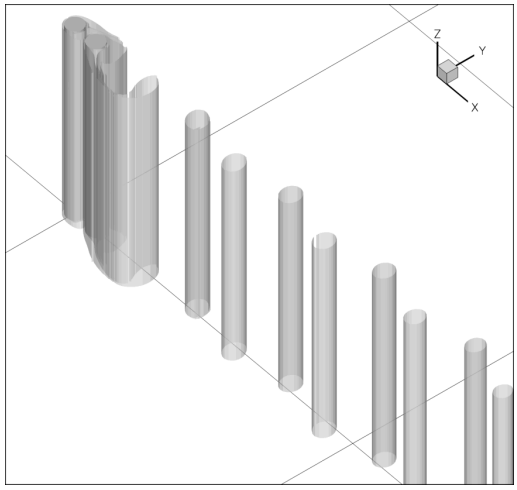

(a) $L_x/D = 1.5$, $Vr = 15.0$

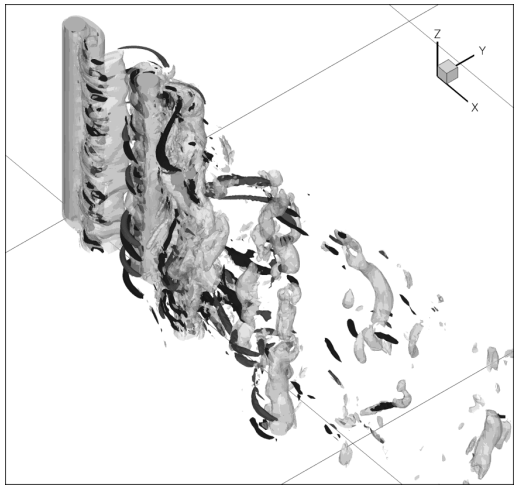

(b) $L_x/D = 5$, $Vr = 8.5$

Figure 10: *Iso-surfaces of spanwise vorticity (transparent) and streamwise vorticity (opaque). Three-dimensional simulations,* $Re = 300$.

states.

For higher reduced velocities, the lift coefficient time history is considerably smoother, but it still shows high energy at frequencies other than the Strouhal frequency, as can be seen in figure 7. The displacement then exhibits strong components at the Strouhal frequency and at a frequency close to the natural frequency.

5. THREE-DIMENSIONAL RESULTS

A few three-dimensional simulations were performed to check the sensitivity of the structural response to three-dimensional structures in the flow. The Reynolds number chosen was 300, which is well beyond the secondary instability in the flow around a single cylinder.

The amplitude results for the configurations $L_x/D = 1.5$, and 5 are shown in figure 9, together with the results obtained from the two-dimensional simulations. In general, the three-dimensional results present the same trend as the two-dimensional ones. However, an important difference between the cases investigated is that, for $L_x/D = 1.5$, the amplitudes of the three-dimensional simulations were higher than those of the two-dimensional simulations, while the inverse occurred for all the other configurations. This difference can be explained if we analyse the vorticity iso-surfaces plotted in figure 10. The configuration $L_x/D = 1.5$ is stable to three-dimensional perturbations at $Re = 300$, hence the resulting flow is actually two-dimensional, as can be seen in figure 10a. Since an increase in the Reynolds number in the two-dimensional flow makes the vortices stronger, the oscillatory forces impinging on the downstream cylinder are also stronger, and this explains why the three-dimensional results gave higher ampli-

tudes than the two-dimensional simulations. On the other hand, for larger separations, the wake is highly three-dimensional, as shown in figure 10b. The presence of three-dimensional structures increases the diffusion of vorticity in the wake and de-correlates the forces in the spanwise direction. These phenomena make the resulting forces on the downstream cylinder less intense, counter-balancing the effect of the increase of the Reynolds number. Consequently, lower amplitudes are observed in the three-dimensional simulations.

6. CONCLUSION

By means of direct numerical simulations, the fluid-structure interaction of the flow past two circular cylinders in a tandem configuration was investigated. , In our model, the upstream body was fixed and the downstream one mounted on an elastic base. The sensitivity of the system to the separation between the cylinders (at $Re = 150$) and to the presence of three-dimensional wake structures (at $Re = 300$) was assessed.

The results showed that there are significant changes in the structural response of the tandem arrangements when compared to an elastically mounted single cylinder. The lock-in region boundaries are completely modified: it is difficult to define an upper limit at smaller separations ($L_x/D \leq 3$) and at larger cylinder separations, the lock-in region is much larger than in the single cylinder case.

The maximum displacement amplitude observed in this region is also higher, approaching values 50% higher than the maximum displacement amplitude of the single cylinder case. In addition, the displacement amplitude responses at high reduced velocities were very significant, in some cases ($L_x/D = 3$) comparable to the highest amplitude in the single cylinder case.

The three-dimensional simulations highlighted that the dynamics of the structural response were not fundamentally affected by the presence of the three-dimensional wake structures. This suggests that two-dimensional simulations might provide some physical insights into preliminary studies of the large parameter space involved in this problem.

7. REFERENCES

J. T. Batina, 1990, Unsteady euler airfoil solutions using unstructured dynamic meshes. *AIAA Journal*, **28** (8): 1381-1388.

A. Beskok and T. C. Warburton, 2001, An unstructured hp finite-element scheme for fluid flow and heat transfer in moving domains. *Journal of Computational Physics*, **174**: 492-509.

B. S. Carmo, 2005, Numerical investigation of the flow around two cylinders in tandem arrangements. Msc dissertation, Escola Politécnica - University of São Paulo, Brazil.

W. Jester and Y. Kallinderis, 2004, Numerical study of incompressible flow about transversely oscillating cylinder pairs. *Journal of Offshore Mechanics and Arctic Engineering - Transactions of the ASME*, **126**: 310-317.

G. E. Karniadakis, 1990, Spectral Element–Fourier methods for incompressible turbulent flows. *Computer Methods in Applied Mechanics and Engineering*, **80**: 367-380.

G. E. Karniadakis and S. J. Sherwin, 2005, *Spectral/hp Element Methods for Computational Fluid Dynamics*. Oxford University Press, 2nd edition.

G. E. Karniadakis, M. Israeli, and S. A. Orszag, 1991 High-order splitting methods for the incompressible Navier–Stokes equations. *Journal of Computational Physics*, **97**: 414-443.

Md. Mahbub Alam, M. Moriya, K. Takai, and H. Sakamoto, 2003, Fluctuating fluid forces acting on two circular cylinders in a tandem arrangement at a subcritical reynolds number. *Journal of Wind Engineering and Industrial Aerodynamics*, **91**: 139-154.

N. M. Newmark, 1959, A method of computation for structural dynamics. *Journal of the Engineering Mechanics Division of ASCE*, **85**: 67-94.

SP Singh and S Mittal, 2005, Vortex-induced oscillations at low reynolds numbers: Hysteresis and vortex-shedding modes. *Journal of Fluids and Structures*, **20**: 1085-1104.

R. H. J. Willden and J. M. R. Graham, 2006, Three distinct response regimes for the transverse vortex-induced vibrations of circular cylinders at low reynolds numbers. *Journal of Fluids and Structures*, **22**: 885-895.